J. Fluid Mech. (1974), *vol.* 65, *part* 1, *pp.* 189–206
Printed in Great Britain

The solution of viscous incompressible jet and free-surface flows using finite-element methods

By R. E. NICKELL, R. I. TANNER AND B. CASWELL
Division of Engineering, Brown University

(Received 9 March 1973 and in revised form 9 February 1974)

We discuss the creation of a finite-element program suitable for solving incompressible, viscous free-surface problems in steady axisymmetric or plane flows. For convenience in extending program capability to non-Newtonian flow, non-zero Reynolds numbers, and transient flow, a Galerkin formulation of the governing equations is chosen, rather than an extremum principle. The resulting program is used to solve the Newtonian die-swell problem for creeping jets free of surface tension constraints. We conclude that a Newtonian jet expands about 13 %, in substantial agreement with experiments made with both small finite Reynolds numbers and small ratios of surface tension to viscous forces. The solutions to the related 'stick–slip' problem and the tube inlet problem, both of which also contain stress singularities, are also given.

1. Introduction

The extrusion of viscous jets is a subject of considerable rheological importance and great analytical difficulty, being a viscous flow problem with a free surface. There are few analytical solutions involving free surfaces and, in those that do exist, some approximation is usually made in order to facilitate the solutions. Typical assumptions, for example, are to postulate a free-surface shape or to assume a small displacement from a known shape. When nothing is known about the shape of the free surface in advance, little progress has been reported. A further complication that arises with mixed boundary-value problems, in general, and the jet-flow problem, in particular, is the presence of a stress singularity at the line of separation (Michael 1958); similar singularities have been discussed by Huh & Scriven (1971) for the problem of a drop wetting a surface. Because of the known difficulties, numerical methods were chosen for the resolution of the viscous jet and similar problems. This paper relates our experiences with this class of problems.

For the case of non-Newtonian fluids, the extrudate is known (Lodge 1964) to expand to perhaps several multiples of the die diameter, giving the 'die-swell' phenomenon. Perhaps less well known is the significant swelling of a purely Newtonian flow emerging from a long tube at sufficiently low Reynolds numbers. This expansion seems to have been discovered experimentally by Middleman & Gavis (1961). They showed that expansion occurred below a Reynolds number of 16, and that contraction was present at higher Reynolds numbers. To account for surface tension effects, a correction formula was given

in this paper, which apparently showed that the effect of surface tension on the final jet diameter was quite important. For example, the final jet diameter, made dimensionless by using the tube diameter, was measured as 1·13 at a Reynolds number of 2. After removing the effect of surface tension by application of the correction formula, the predicted final dimensionless diameter of a surface-tension-free jet was only 1·07. Subsequently, however, two amendments were made to the correction formula, and the final one (Gavis 1964) showed that scarcely any correction to the original measured data was needed, and consequently the expansion for a surface-tension-free jet at a Reynolds number of 2 would be close to 13 %. Confirmation of these results was provided by Goren & Wronski (1966), who showed experimentally that the effect of surface tension on the final jet diameter was quite weak. For example, changing the surface tension parameter S (defined to be $\rho\sigma D/\eta^2$) from 0·45 to 0·054 at a Reynolds number of about 4 produced no significant change in the expansion ratio, which was about 10 %. Here ρ is the fluid density, σ the surface tension, D the tube diameter and η the fluid viscosity. The mean jet velocity $\bar{u}$ will be taken as a characteristic speed, and thus the Reynolds number Re is defined to be $\rho\bar{u}D/\eta$. The parameter S, which does not depend on $\bar{u}$, is recognized as the product of Re and $\sigma/\eta\bar{u}$, the latter group giving a measure of the ratio of surface tension forces to viscous forces in the flow. Thus, when $S/Re \ll 1$, we may expect the effect of surface tension forces to be negligible.

In the experiments of Goren & Wronski (1966), a variation of S/Re from about 0·1 to 0·01 produced no significant effect on the final jet diameter at a Reynolds number of 4. To obtain results at a lower Reynolds number, one of the present authors (in some unpublished work dating from 1965) made some experiments in which a 1000-poise silicone liquid was slowly extruded through a $\frac{1}{4}$ inch diameter tube into a bath containing a mixture of kerosene and carbon tetrachloride of matching density. Thus problems with gravitational forces were eliminated, and the interfacial tension, inertia and external viscous forces were very small compared with the viscous forces in the jet itself. The external bath viscosity was about 10^{-4} of the jet velocity, S was about 10^{-5} and Re was about 10^{-3}, yielding an expansion of 13 ± 1 %. A much more extensive set of experiments at very low Reynolds and S numbers was performed by Batchelor & Horsfall (1971), who also used extrusion into a bath of matching density to avoid problems with gravitational forces. For a Newtonian fluid with a viscosity of 10^5 poise, they reported a mean swelling of 13·5 %. We consider these experiments to be the most useful in defining the jet shape under conditions when Re and S/Re approach zero.

Thus there seems to be a limiting swelling ratio in the absence of inertial and surface tension effects. Apparently this is not obvious; and Richardson (1970*a*), unaware of any experiments at Reynolds numbers below 2, suggested that there might not be *any* jet-type flow in a strictly creeping flow, and that the very concept of a jet is one requiring inertia. His argument is that one might expect the fluid to fill all space on emerging from a tube if the tendency, due to inertia, of the fluid to continue in a state of uniform motion is removed. But, even without inertia, it seems possible to us that a jet-like form might occur in a creeping flow, if the choice between it and a space-filling flow is available, and, for example,

a lower rate of energy dissipation resulted from the jet-like form. (These rates of energy dissipation are compared at the end of § 5.) We are also not convinced by the argument from mass and momentum balances (Richardson 1970*a*), which appears to show that no free Newtonian jet (no gravity, backpull on the jet or surface tension considered) can expand unless the total axial force at the jet exit is negative. This would imply that a strictly inertialess jet cannot expand, since the total axial exit force is then exactly zero.

In fact, Richardson's arguments break down when we consider strictly creeping flows, since the momentum balance then does not involve the final jet diameter and velocity and, therefore, no bound on the die-swell can be found from his method. The boundary-value problem must be solved directly in this case. An expansion in powers of the Reynolds number, as attempted by Richardson, does not circumvent the difficulty. He shows that the estimate of swelling at zero Reynolds number involves a coefficient that only appears in the first-order perturbation (the coefficient being multiplied by the Reynolds number). The coefficient cannot be ignored in attempting to calculate die-swell at zero Reynolds number if a momentum balance is used. We fail to see how the presence of this coefficient in the swelling ratio suggests non-uniqueness for creeping flows; it seems rather that one cannot determine the swelling from momentum considerations for strictly creeping flows.

Nevertheless, we have found the two papers by Richardson (1970*a*, *b*) very useful, as will be seen below, and our work might be considered as a computer experiment to test some of these ideas. The main consideration, however, is of broader scope, and consists of presenting an efficient computational method that is well adapted to the solution of incompressible viscous flow problems with mixed boundary conditions and unknown free surfaces.

The main computational difficulty is the unknown free surface, on which we require simultaneously that the normal stress, the shear stress and the normal velocity are zero. (If surface tension is retained, the boundary conditions are more complex; here we do not consider these complications, although it is hoped to do so in future computations.) Hence, we shall restrict the present discussion to zero Reynolds numbers and Newtonian flow, although the computational scheme is perfectly general in this regard. At present, the program is limited to steady plane and axisymmetric flows.

When the literature on computational methods in fluid mechanics is examined, the overwhelming tendency is to use a stream function for the incompressible axisymmetric/plane flow class of problems. Generally speaking, the sequence of calculations is to find the stream function first and recover the pressure in a separate computation. For free-surface viscous flow problems, this procedure is most inconvenient, since the free boundary conditions are given in terms of the stress components, which involve the pressure explicitly. Furthermore, double differentiation of the stream function (to find the stresses) is a numerically noisy operation and should be avoided where possible. Another alternative is the MAC method, and a satisfactory solution of the exact free-surface boundary condition, using this approach, can be traced from the work of Pracht (1971). We shall not use the MAC method here, primarily because the method is somewhat wasteful,

in terms of computational effort, for our class of problems, and we view cost as an essential aspect of our numerical work. In agreement with Pracht (1971), however, the velocity components and the pressure are chosen as primitive computational variables for the convenient treatment of free-surface problems. Either finite-difference or finite-element methods can then be used to discretize the governing equations. The former are more widely used in fluid mechanics computations, but they involve annoying difficulties in the satisfaction of boundary conditions or irregular or unknown boundary meshes. For this reason, the finite-element approach, which largely avoids these difficulties, was implemented.

The finite-element method has received considerably less application in fluid mechanics than in solid mechanics. In the latter field, for example, an insistence upon strict incompressibility is comparatively rare, and few examples of application are seen in the literature, save for specialist publications, such as those sponsored by the solid propellent rocket industry. Herrmann (1965) produced a variational scheme that is a suitable basis for an incompressible finite-element program, and could be regarded as a theoretical foundation for Stokes flow problems. For general creeping flows, solutions using finite elements have been given by Atkinson *et al.* (1969, 1970) and by Thompson, Mack & Lin (1969). Chan & Larock (1973) have investigated potential jets. The latter two permit free surfaces in the flow field, but neglect either viscosity or inertia; uniquely, velocities and pressure are used as primitive variables. While Thompson *et al.* (1969) are not quite clear about whether Lagrangian or Eulerian spatial coordinates are being used, one must really divide the *space* containing the material into finite elements when adopting the usual Eulerian formulation for the Navier–Stokes equations. The finite elements are not now discrete pieces of material always composed of the same fluid particles, as in a Lagrangian solid mechanics formulation; instead, the particles flow through the elements. Apart from some potential flow and lubrication studies and the work of Olson (1972), Oden & Wellford (1972), Cheng (1972) and Taylor & Hood (1973), mentioned again below, we are unaware of any other relevant, published work on fluid mechanics that actually exhibits problem solutions (including inertia effects) using finite elements, and further exploration is indicated.

It is worth pointing out, at this time, that the finite-element method is a generalization (in terms of the ease of construction of approximating sequences) of the Galerkin method discussed by Orszag (1971), Fox & Deardorff (1972) and others.

In §2 we discuss the basic theoretical approach, and §3 describes the program. Finally, §§4 and 5 exhibit solutions to the free jet and other problems.

2. Basic analytical principles

For the general formulation we shall simply let the flow be steady; we shall not restrict ourselves to plane or axisymmetric flows at this stage. In a Cartesian tensor representation we have the conservation laws

$$\frac{\partial t_{ij}}{\partial x_j} + \rho\left(f_i - \frac{Dv_i}{Dt}\right) = 0, \tag{2.1}$$

$$\frac{\partial v_i}{\partial x_i} = 0, \tag{2.2}$$

where v_i are the velocity components in the direction of x_i, f_i are the body force components, and t_{ij} are the stress components; Dv_i/Dt signifies, for steady flow, the acceleration $v_j \partial v_i/\partial x_j$. A constitutive equation is necessary, and here we are concerned only with the Newtonian case

$$t_{ij} = -p\delta_{ij} + \eta\left(\frac{\partial v_i}{\partial x_j} + \frac{\partial v_j}{\partial x_i}\right), \tag{2.3}$$

where p is the pressure and δ_{ij} are the components of the unit tensor.

Boundary conditions are given on the components of v_i over part of the boundary (S_v) and traction, or stress, boundary conditions over the rest of the boundary (S_t); the entire boundary is $S = S_v + S_t$. On S_t we shall assume

$$t_{ij} n_j = T_i, \tag{2.4}$$

where the T_i are given and n_j is the outward-pointing normal unit vector on the surface.

As is well known, and has been re-emphasized recently (Finlayson 1972), no extremum principle of the classical type exists for this problem. Hence the conventional methods for formulating the finite-element equations fail (Zienkiewicz 1971). An alternative is the Galerkin method (Kantorovich & Krylov 1964; Szabo & Lee 1969; Zienkiewicz & Taylor 1972), or the related energy-balance ideas of Oden (1970) and Oden & Wellford (1972). Olson (1972) has given finite-element solutions of the Navier–Stokes equations through the use of a restricted variational method with a stream function; Cheng (1972) also uses a stream function. Taylor & Hood (1973) have solved some problems involving time dependence and inertia forces. They have not considered problems with free surfaces and stress singularities, however, and no comparison is available between their computed results for drag on a cylinder and corresponding experimental results. Thus the accuracy of their method in the complex problems considered in the present paper is unknown; the work of Oden & Wellford (1972) also does not consider free surfaces.

To use the Galerkin method, we assume that the solution vector $\langle v_i, p\rangle$ can be expressed in the form

$$\begin{Bmatrix} v_i \\ p \end{Bmatrix} = \begin{Bmatrix} v_i^* \\ p^* \end{Bmatrix} + \sum_{m=1}^{M} \begin{Bmatrix} a_{im} u_{im} \\ b_m \phi_m \end{Bmatrix}, \tag{2.5}$$

where $\langle v_i^*, p^*\rangle$ is a particular integral of the system satisfying the boundary conditions on S_v, the a_{im} and b_m are unknown constants, and the u_{im} and ϕ_m are a set of 'trial' functions satisfying zero velocity boundary conditions on S_v (but not necessarily the stress boundary conditions on S_t). The trial functions are assumed to form a complete set of functions over the fluid-filled space. If (2.1) and (2.2) are arranged in vector form as an operator on $\langle v_i, p\rangle$ and the assumed solution (2.5) is inserted therein, a residual vector $\mathbf{R}$ is obtained since, in general, the trial functions will not satisfy the conservation equations exactly. The Galerkin process then makes each element of $\mathbf{R}$ orthogonal to each corresponding

element of the M vectors $\{u_{im}, \phi_m\}$ in turn, giving $4M$ equations for the $4M$ unknowns a_{im}, b_m. Thus we find

$$\int_v \left\{\frac{\partial t_{ij}}{\partial x_j} + \rho\left(f_i - \frac{Dv_i}{Dt}\right)\right\} u_{im}\, dV = 0 \quad (i \text{ not summed}; \quad m = 1, \ldots, M), \tag{2.6}$$

and

$$\int_v \frac{\partial v_j}{\partial x_j}\, \Phi_m\, dV = 0 \quad (m = 1, \ldots, M). \tag{2.7}$$

Use of the divergence theorem on the first part of (2.6), using (2.4) and the vanishing of u_{im} on S_v, yields

$$-\int_v t_{ij} \frac{\partial u_{im}}{\partial x_j}\, dV + \int_{s_t} T_i u_{im}\, dS + \int_v \rho\left(f_i - \frac{Dv_i}{Dt}\right) u_{im}\, dV = 0$$
$$(i \text{ not summed}; \quad m = 1, \ldots, M). \tag{2.8}$$

This form, with (2.7), is the basis of the method used by Taylor & Hood (1973) and Oden & Wellford (1972). The reduction of the order of the differential operator is characteristic of the finite-element method, and permits the use of trial functions which are only once differentiable. We shall retain (2.7), which gives M linear equations for the a_{im}, but a more symmetrical form than (2.8) will be used in the present treatment. To find this form, multiply each of the components of (2.8) by an arbitrary constant, α_{im} say, and sum over i and m. Defining

$$\delta v_i = \sum_{m=1}^{M} \alpha_{im} u_{im}, \tag{2.9}$$

we may now rewrite the sum over (2.8) as

$$0 = -\tfrac{1}{2}\int_v t_{ij}\left(\frac{\partial \delta v_i}{\partial x_j} + \frac{\partial \delta v_j}{\partial x_i}\right) dV + \int_{s_t} T_i \delta v_i\, dS + \int_v \rho\left(f_i - \frac{Dv_i}{Dt}\right) \delta v_i\, dV. \tag{2.10}$$

This is now formally identical (except for the $(Dv_i/Dt)/Dt$ term) to the variational equation of Thompson *et al.* (1969). Since all the α_{im} are arbitrary, (2.10) may be split into $3M$ equations for the α_{im}, b_m by the process used in that paper. The details of the reduction to separate components is discussed in §3. The advantage of the present formulation is that, for the case of creeping flow, the numerical procedure is based on an extremum principle. In general, if Dv_i/Dt is not neglected, the equations for the α_{im}, b_m are nonlinear; for Stokes flow, they are linear. Note also that, in two important special cases, the surface integrals in (2.10) vanish (it is always supposed that the trial functions satisfy the essential boundary conditions on v_i): (i) when the surface tractions vanish; and (ii) when the fluids 'slips' without shear stress along a fixed boundary (Richardson 1970*a*).

3. The finite-element program

The computer program, called AXFINR, is a system of FORTRAN routines that can be used to solve, approximately, axisymmetric or plane fluid mechanics problems having a free-surface boundary condition, with a viscosity that may depend upon the rate of deformation, and including an Oseen-type approximation to the convective acceleration terms. By 'Oseen-type approximation', we mean that, at each stage in the iterative procedure, in the nonlinear convective terms in the acceleration, we set $v_j \partial v_i/\partial x_j$ equal to $v_j^0 \partial v_i/\partial x_j$, where v_j^0 is the best

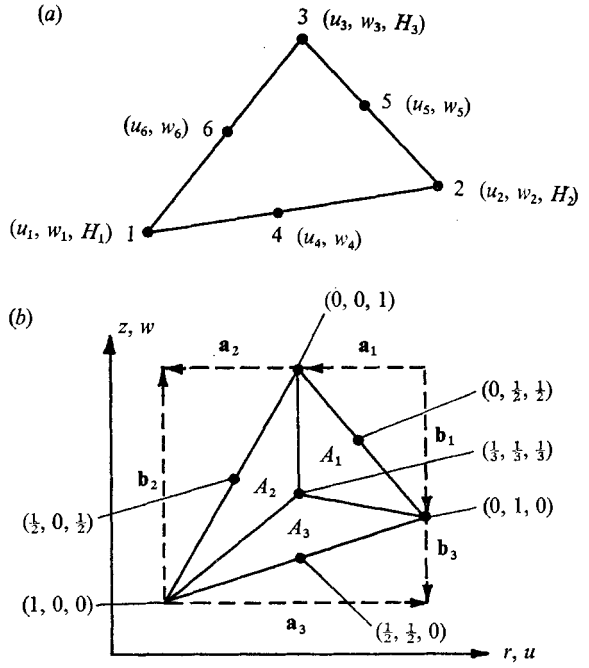

FIGURE 1. (*a*) Linear strain triangle nodal variables.
(*b*) Triangular co-ordinate system.

available known estimate of v_j. The original version of the program was conceived (Schkade 1970) for solving elasticity boundary-value problems for solid materials that were incompressible or nearly incompressible, using the mixed variational principle of Herrmann (1965) that introduced a quantity H proportional to the mean tension as a primary variable, in addition to the displacement field. This version has been modified to include an iterative procedure for the free-surface boundary condition and the nonlinearities associated with non-Newtonian flow and non-zero Reynolds numbers. The following discusses only the detailed points peculiar to AXFINR; for a general discussion of the construction of finite-element programs see Zienkiewicz (1971).

The basic finite element is a 20 degree-of-freedom general quadrilateral composed of four 15 degree-of-freedom triangles (for axisymmetric problems, this should be thought of as an axisymmetric ring of quadrilateral cross-section). For each of the triangular subelements, the velocity components are expressed as quadratic functions of the spatial variables, while the mean tension is assumed to be a linear function (an adjunct program that is used to compute temperature distributions in the fluid invokes a linear assumption for the scalar temperature field, as well). The arrangement of nodal point variables is shown in figure 1 (*a*). After matrix assembly of the contributions from the four triangles, the eleven interior degrees of freedom associated with the common midside nodes and the quadrilateral centroid are condensed from the system. After the solution has been obtained for the retained degrees of freedom, these interior quantities can be found, since the elimination operations are normally saved for later use.

A convenient procedure for developing the triangular subelement stiffness-rate matrix and load vector is to consider a co-ordinate transformation on the spatial variables (r, z) to a set of triangular co-ordinates (or area co-ordinates, as they are sometimes called: Felippa 1965). Referring to figure 1(*b*), the area co-ordinates $(\zeta_1, \zeta_2, \zeta_3)$ are given by

$$\zeta_i = A_i/A \quad (i = 1, 2, 3), \tag{3.1}$$

where A is the total area of the triangle. Note that the quantities a_1, b_1, etc. can be thought of as vector components, and that the area can be found from

$$2A = a_j b_i - a_i b_j, \tag{3.2}$$

where i and j denote two vertices of the triangle. Also note that $\sum_{i=1}^{3} a_i = \sum_{i=1}^{3} b_i = 0$, and that $\zeta_1 + \zeta_2 + \zeta_3 = 1$. The transformation can thus be expressed by

$$2A\zeta_i = 2A_i + b_i r + a_i z, \tag{3.3}$$

and its inverse can be cast in matrix form as

$$\begin{Bmatrix} 1 \\ r \\ z \end{Bmatrix} = \begin{bmatrix} 1 & 1 & 1 \\ r_1 & r_2 & r_3 \\ z_1 & z_2 & z_3 \end{bmatrix} \cdots \begin{Bmatrix} \zeta_1 \\ \zeta_2 \\ \zeta_3 \end{Bmatrix}. \tag{3.4}$$

From (3.3), the spatial derivatives are seen to be

$$\frac{\partial \zeta_i}{\partial r} = b_i/2A, \quad \frac{\partial \zeta_i}{\partial z} = a_i/2A, \tag{3.5}$$

and, from (3.4),

$$\frac{\partial r}{\partial \zeta_i} = r_i, \quad \frac{\partial z}{\partial \zeta_i} = z_i. \tag{3.6}$$

Functions, and their derivatives, that are to be interpolated over the triangle can be found from the expression

$$f(\zeta_i) = \mathbf{f}^{0T} . \mathbf{h}(\zeta_i), \tag{3.7}$$

where the vector $\mathbf{f}^0$ represents the nodal point values of the function and the vector $\mathbf{h}(\zeta_i)$ indicates either linear or quadratic interpolation. For the mean tension variable

$$\mathbf{h}^T(\zeta_i) = \langle \zeta_1, \zeta_2, \zeta_3 \rangle, \tag{3.8}$$

whereas, for the velocity components,

$$\mathbf{h}^T(\zeta_i) = \langle \zeta_1(2\zeta_1 - 1), \zeta_2(2\zeta_2 - 1), \zeta_3(2\zeta_3 - 1), 4\zeta_1\zeta_2, 4\zeta_2\zeta_3, 4\zeta_3\zeta_1 \rangle. \tag{3.9}$$

With these preliminaries in mind, define a vector composed of the functions to be interpolated

$$\mathbf{v}^T(\zeta_i) = \langle u, w, H \rangle, \tag{3.10}$$

where u is the radial component of velocity, w is the axial component of velocity and H is the mean tension normalized by a reference viscosity, η_0†. Given that the vector of nodal point unknowns $\mathbf{v}^0$ is arranged so that

$$\mathbf{v}^{0T} = \langle u_1, w_1, H_1, u_2, w_2, H_2, u_3, w_3, H_3, u_4, w_4, u_5, w_5, u_6, w_6 \rangle, \tag{3.11}$$

† H is related to the pressure p by the rule $H = -p/\eta_0$.

the interpolation polynomial terms can be arranged so that

$$\mathbf{v}(\zeta_i) = \boldsymbol{\alpha}(\zeta_i) \cdot \mathbf{v}_0. \tag{3.12}$$

In a similar manner, define a vector composed of derivatives of the velocity field and the mean pressure

$$\boldsymbol{\epsilon}^T(\zeta_i) = \left\langle \frac{\partial u}{\partial r}, \frac{u}{r}, \frac{\partial w}{\partial z}, \frac{\partial u}{\partial z}, \frac{\partial w}{\partial r}, H \right\rangle, \tag{3.13}$$

and note that, using (3.5),

$$\boldsymbol{\epsilon}(\zeta_i) = \boldsymbol{\beta}(\zeta_i) \cdot \mathbf{v}_0. \tag{3.14}$$

The Galerkin method, as applied to this class of problems, then yields

$$\int_V [\delta\boldsymbol{\epsilon}^T \cdot \mathbf{D} \cdot \boldsymbol{\epsilon} - \delta\mathbf{v}^T \cdot \mathbf{B}] r\, dr\, d\theta\, dz = \int [\delta\mathbf{v}^T \cdot \Upsilon]\, dS, \tag{3.15}$$

where the symbol δ refers to the trial function corresponding to a particular quantity; Υ and $\mathbf{B}$ denote the prescribed boundary traction vector and the equivalent body force vector, respectively; and $\mathbf{D}$ is a constitutive matrix given by

$$\mathbf{D} = \eta \begin{bmatrix} 2 & 0 & 0 & 0 & 0 & \frac{1}{2} \\ 0 & 2 & 0 & 0 & 0 & \frac{1}{2} \\ 0 & 0 & 2 & 0 & 0 & \frac{1}{2} \\ 0 & 0 & 0 & \frac{1}{2} & \frac{1}{2} & 0 \\ 0 & 0 & 0 & \frac{1}{2} & \frac{1}{2} & 0 \\ \frac{1}{2} & \frac{1}{2} & \frac{1}{2} & 0 & 0 & 0 \end{bmatrix}. \tag{3.16}$$

all $\frac{1}{2}$'s should be 1

JFM 67 p828

The matrix $\mathbf{D}$ is written for the special case of incompressibility, but is easily generalized to include fluid compressibility, if required. The equivalent body force vector $\mathbf{B}$ can be decomposed into

$$\mathbf{B} = \rho(\mathbf{f} - \mathbf{a}), \tag{3.17}$$

where ρ is the density, $\mathbf{f}$ is the body force vector, and $\mathbf{a}$ is the acceleration vector. With an Oseen-type approximation, the latter term can be written as

$$\int_v [\delta\mathbf{v}^T \cdot \boldsymbol{\phi}_1 \cdot \mathbf{v} + \delta\mathbf{v}^T \cdot \boldsymbol{\phi}_2 \cdot \mathbf{v}] r\, dr\, d\theta\, dz, \tag{3.18}$$

where $\boldsymbol{\phi}_1$ and $\boldsymbol{\phi}_2$ are operational matrices given by

$$\boldsymbol{\phi}_1 = \begin{bmatrix} \rho u^0 \frac{\partial}{\partial r} & 0 & 0 \\ 0 & \rho w^0 \frac{\partial}{\partial z} & 0 \\ 0 & 0 & 0 \end{bmatrix}, \tag{3.19}$$

$$\boldsymbol{\phi}_2 = \begin{bmatrix} \rho w^0 \frac{\partial}{\partial z} & 0 & 0 \\ 0 & \rho u^0 \frac{\partial}{\partial r} & 0 \\ 0 & 0 & 0 \end{bmatrix}. \tag{3.20}$$

Carrying out the volume and surface area integration indicated in (3.5) and (3.18) (note that closed form integration is not feasible for the most general case,

thereby giving rise to numerical (Gaussian) integration), the governing matrix equation for the element can be written as

$$(\mathbf{K}+\mathbf{M}_1+\mathbf{M}_2).\mathbf{v}_0 = \mathbf{F}, \tag{3.21}$$

where

$$\mathbf{K} = \int_V \boldsymbol{\beta}^T \mathbf{D} \boldsymbol{\beta}\, dV, \quad \mathbf{M}_1 = \int_V \boldsymbol{\alpha}^T \boldsymbol{\phi}_1 \boldsymbol{\alpha}\, dV, \quad \mathbf{M}_2 = \int_V \boldsymbol{\alpha}^T \boldsymbol{\phi}_2 \boldsymbol{\alpha}\, dV, \tag{3.22}$$

and

$$\mathbf{F} = \int_V \boldsymbol{\alpha}^T \mathbf{f} dV + \int_{S_t} \boldsymbol{\alpha}^T \boldsymbol{\Upsilon}\, dS.$$

A careful examination of $\mathbf{M}_1$ and $\mathbf{M}_2$ reveals that, in general, both are asymmetric. This leads to a number of interesting computational choices, which will be reported upon in later work: (i) the assembled equations can be solved as an asymmetric system; (ii) both $\mathbf{M}_1$ and $\mathbf{M}_2$ can be placed on the right-hand side of (3.21) and multiplied by the nodal point vector of the previous iteration; or (iii) some combination of the two. In this case, we selected the last option and formed the matrices

$$\mathbf{M}_1^* = \tfrac{1}{2}(\mathbf{M}_1^T + \mathbf{M}_1 + \mathbf{M}_2^T + \mathbf{M}_2) \tag{3.23}$$

and

$$\mathbf{M}_2^* = \tfrac{1}{2}(\mathbf{M}_1 - \mathbf{M}_1^T + \mathbf{M}_2 - \mathbf{M}_2^T), \tag{3.24}$$

then the matrix equation for the 'kth' iteration becomes

$$(\mathbf{K}+\mathbf{M}_1^*).\mathbf{v}_0^{(k)} = \mathbf{F} - \mathbf{M}_2^*.\mathbf{v}_0^{(k-1)}. \tag{3.25}$$

4. Creeping flow solutions without free surfaces

Because of the refined finite element used, solutions to Poiseuille flow are essentially exact, giving errors of order 10^{-6} on the primitive variables (IBM 360/67 computer, selective double-precision arithmetic). A more exacting test is a flow problem with stress singularities in the field. Two such problems are discussed here, in order to demonstrate the accuracy available for both overall quantities and local variables.

A problem of interest in viscometry (Weissberg 1962) concerns the pressure drop, in excess of that due to Poiseuille flow, at the entrance of a sharp-edge tube (figure 2). No analytical or accurate numerical solutions are known, to us, that give the details of the flow field; however, Weissberg's (1962) variational calculation of the excess pressure drop is believed to give an accurate bound that is useful for comparison with our computed values. He has concluded that the extra pressure drop for the inlet problem is near to

$$\Delta P_e = 3{\cdot}00\eta Q/2R_0^3, \tag{4.1}$$

where Q is the total flow rate, R_0 is the tube radius, and η is the fluid viscosity.

For the finite-element solution, 150 elements (1000 equations) were used to model the field. It should be noted that, in general, infinite or semi-infinite regions must be dealt with in such problems. In order to economize on the size of the field to be computed, we have used knowledge of the eigenvalues governing the extinction of disturbances in creeping flows between plane walls or in tubes (Tanner 1963; Waldron 1966; Zidan 1969). Generally speaking, these disturbances

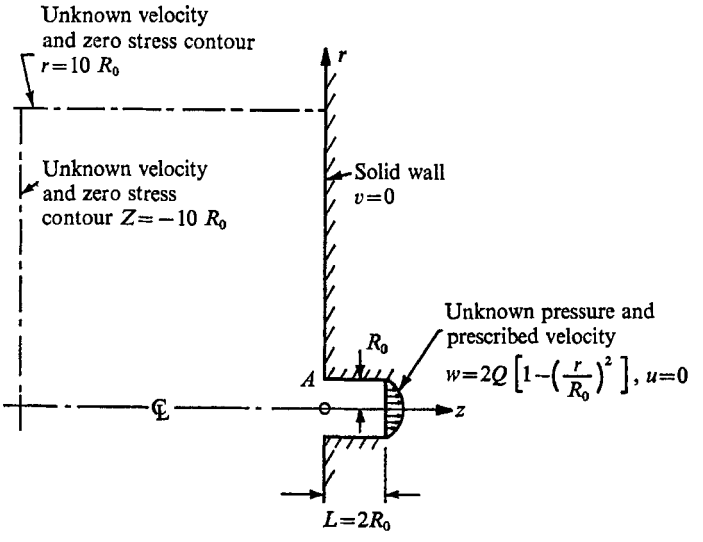

FIGURE 2. Inlet problem, with stress singularity at A.

will be attenuated by a factor of about e^{-6} to e^{-9} in a flow distance of one diameter, or width, and, therefore, the computing fields can be of commensurate length. In this way, we computed the pressure drop between the exit plane and the zero-stress contour (figure 2), finding

$$\Delta P_e = 2{\cdot}999\eta Q/2R_0^3. \tag{4.2}$$

This remarkably accurate result was insensitive to mesh adjustments, although the stress and velocity fields were not of comparable accuracy, especially near the stress singularity at the inlet corner A.

In order to exhibit the details of the stress field near a singularity, we considered the plane, creeping-flow, 'stick–slip' problem (figure 3(*a*)). Richardson (1970*a*, *b*), in an investigation of die-swell, used integral transform techniques to solve this problem, and provided sufficient numerical details to allow an assessment of the accuracy of our program. The element pattern used in our investigation is shown in figure 3(*a*); 135 elements are shown. The sketch (figure 3(*b*)) shows how the stick–slip condition was modelled. The two smallest elements have lengths of 0·04 units (1 unit = channel half-width), and, as seen in figure 1(*a*), boundary conditions on velocities can be imposed at the midsides of elements, in addition to the vertices. This implies that the origin of the singularity can be located precisely.

This singularity is the dominant feature that we wish to examine in our numerical approximation. According to Richardson, the strength of the singularity is such that the x component of velocity behaves as

$$u(x, 1) \sim 1{\cdot}62\sqrt{x} \quad \text{for} \quad x \to 0^+. \tag{4.3}$$

Thus, the singularity is of the form given by Michael (1958). The computed dimensionless velocity is plotted, in figure 4(*a*), as a function of distance downstream from the singularity and the agreement with Richardson's results is

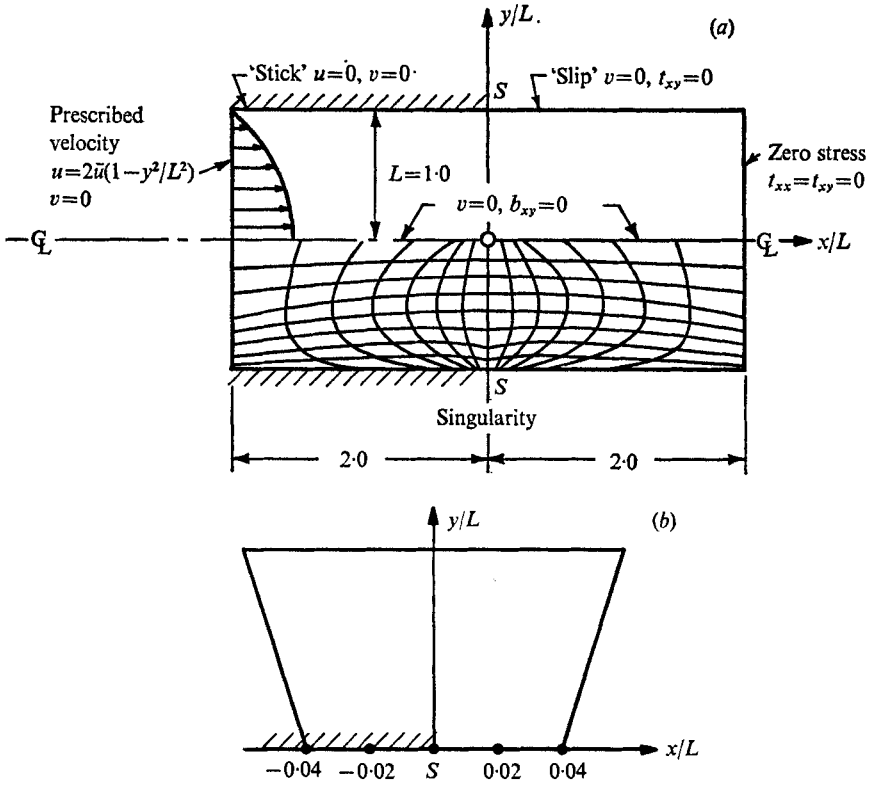

FIGURE 3. (*a*) Stick–slip problem, showing element pattern and boundary conditions. Along centre-line, slip conditions were specified, halving the field. All distances scaled using channel half-width L as unit. (*b*) Details of boundary conditions imposed at nodes in neighbourhood of singularity S. Points left of S, and S itself, have 'stick' boundary conditions, others 'slip', beginning at $x/L = 0{\cdot}02$.

striking, even for the velocity at the first midside node ($x = 0{\cdot}02$). The velocity elsewhere in the field is too close to the Richardson solution to justify graphical comparison.

A more severe test of the program is to consider the other detailed results given by Richardson, notably the centre-line pressure and the normal stress on the 'slip' part of the wall. The former is closely calculated (figure 4(*b*)), and the latter (figure 4(*c*)) given adequately. It should be noted that, near the origin, the component t_{yy} at the wall is the only non-singular stress component and thus the latter test is very severe. For many problems, the indicated accuracy is adequate to handle the singularity; it would of course be possible to refine the mesh by resolving the problem near the singularity to get more accuracy. Consideration was also given to the idea of inserting a special element containing the right kind of singular behaviour; this has the disadvantage that one needs to know what kind of singularity to feed in in advance, and also needs much more special programming. Hence we have not used special elements here, as it is anticipated that they would be very cumbersome in future non-Newtonian com putation.

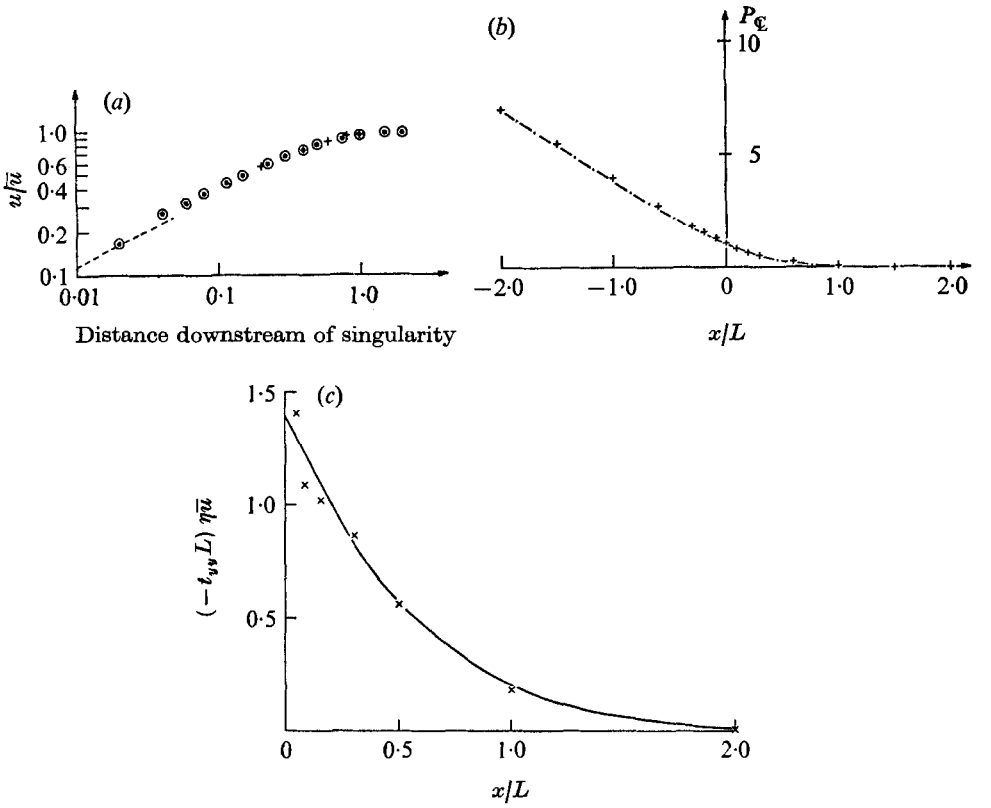

FIGURE 4. Comparison of analytical solution with (*a*) dimensionless velocity field along slip wall (in computed solution $\bar{u} = 1{\cdot}0$); (*b*) dimensionless pressure along duct centre-line P_c, $y = 0$ (pressure made dimensionless using a pressure $\eta\bar{u}/L$, where L is channel half-width, and $\eta\bar{u}/L$ is 1·0 in the computed solution); (*c*) dimensionless normal thrust $-t_{yy}L/\eta\bar{u}$ on slip wall.

	(*a*)	(*b*)	(*c*)
Richardson (1970*b*) analytical solution	+	—·—	——
Computed, 135 elements	⊙	+	×
Asymptotic value (equation (4.3))	- - - -		

We have also computed the results for the axisymmetric version of the stick–slip problem; they are very similar in character to the plane problem. It appears that the strength of the singularity is closely related to the upstream shear rate: in (4.3) the magnitude of the dimensionless upstream shear rate is 3; in our axisymmetric problem the shear rate and the singularity strength were about $\frac{4}{3}$ of those in the plane case.

5. Solution of the Newtonian die-swell problem and comparison with experiments

Because of the weak effect of surface tension and the interest in seeing if there is a steady jet flow in the limiting case, we shall only present here the results for creeping jets without surface tension. The only comparable calculations known

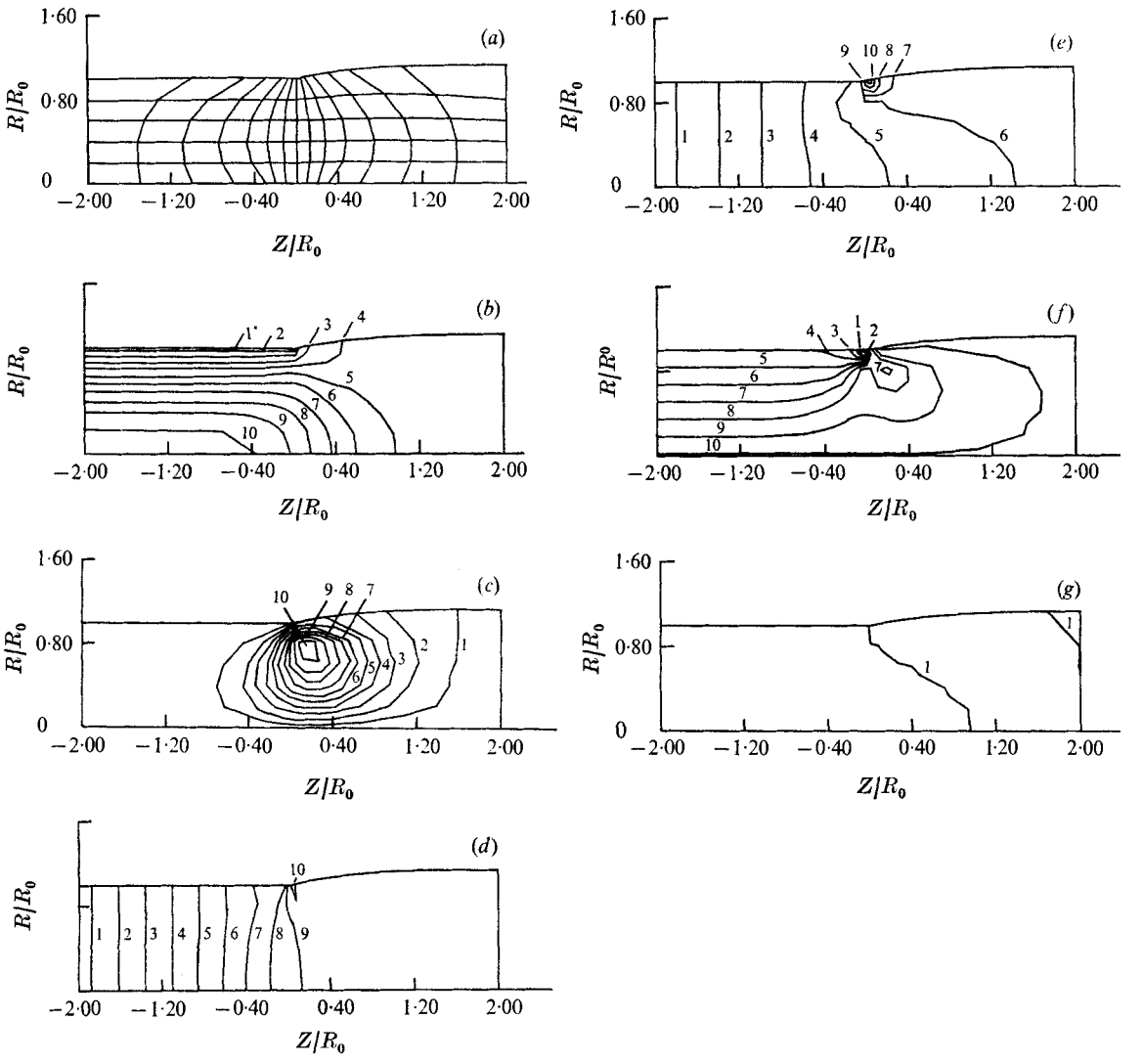

FIGURE 5. Newtonian jet (*a*) problem mesh pattern, (*b*) axial velocity contours, (*c*) radial velocity contours, (*d*) jet radial stress $t_{rr}R_0/\eta\bar{u}$ contours, (*e*) axial stress $t_{zz}R_0/\eta\bar{u}$ contours, (*f*) shear stress $t_{rz}R_0/\eta\bar{u}$ contours, (*g*) zero-pressure contour (positive pressure at centre-line). Values on contours correspond to dimensionless velocities ((*b*) and (*c*)) and stresses ((*d*)–(*f*)), as follows.

	(1)	(2)	(3)	(4)	(5)
(*b*)	0·1	0·3	0·5	0·7	0·9
(*c*)	0·014	0·042	0·070	0·098	0·126
(*d*)	−17	−15	−13	−11	−9
(*e*)	−16·4	−13·1	−9·9	−6·7	−3·4
(*f*)	−6·0	−5·3	−4.7	−4·0	−3·4

	(6)	(7)	(8)	(9)	(10)
(*b*)	1·1	1·3	1·5	1·7	1·9
(*c*)	0·154	0·182	0·210	0·238	0·266
(*d*)	−7	−5	−3	−1	1
(*e*)	−0·2	3·1	6·3	9·6	12·8
(*f*)	−2·7	−2·0	−1·4	−0·7	0

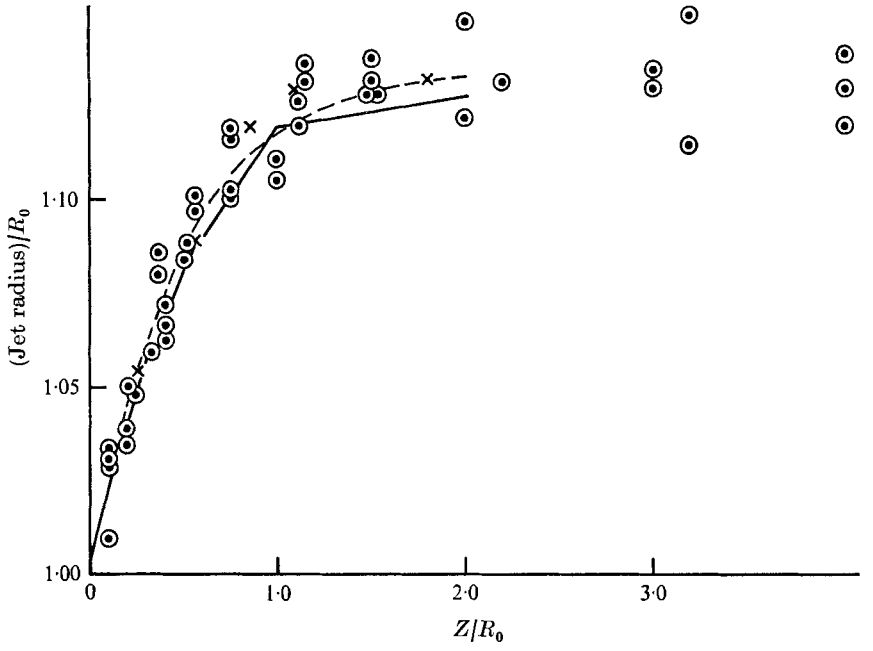

FIGURE 6. Comparison of computed jet shape (——) with our own experiments (×) and those of Batchelor & Horsfall (1971) (⊙). In all cases $Re < 10^{-3}$, and surface tension parameter $\rho\sigma R_0/\eta^2 < 10^{-5}$. The equation of the least-squares fitted curve is $R/R_0 = +0{\cdot}135\,(1-\exp -2{\cdot}067/R)$.

to us are the unsatisfactory attempts of Horsfall (1971) and Waldron (1966). Since the jet profile is initially unknown, iteration is necessary. On the free surface we have the simultaneous requirement that the stress vector is zero (taking ambient pressure as given and ignoring air drag) and the velocity normal to the surface is zero. The successful iteration scheme used prescribes a shape with zero stress boundary conditions and computes the velocity field. In general, we shall not have prescribed a stream surface, and the normal velocity will not be zero. A new stream surface can now be computed, starting from a known fixed point (the tube lip in the jet problem) and the process repeated until it converges. Typically 4 iterations were adequate for the jet problem; for example, final dimensionless diameters of 1·116, 1·126, 1·128, 1·128 were obtained successively starting from a diameter of 1·000. Contour plots are automatically drawn for any of 17 variables. In figures 5(*b*)–(*g*) we show the results for the fields v_z, v_r, t_{rr}, t_{zz}, t_{rz} and the zero contour of p. The element pattern, shown in figure 5(*a*), was similar to that used for the stick–slip problem. In these plots, velocities are made dimensionless using the mean axial flow rate $\bar{u}$, and the stresses are made dimensionless by using $\eta\bar{u}/R_0$; thus, at the wall far inside the tube, the dimensionless shear stress is $-4{\cdot}0$. (The contour values in the figure captions are dimensionless.) We see that the Newtonian die-swell is about 13 %. A comparison of the jet shape from experiments (Batchelor & Horsfall 1971) and the computation is shown in figure 6; our own unpublished experiments on silicone fluid, mentioned in §1, are marked with crosses. Interfacial tension, inertia, and external drag

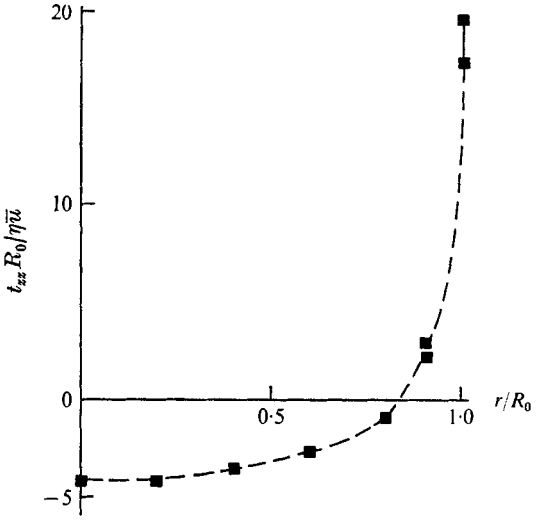

FIGURE 7. Dimensionless tensile stress $t_{zz}R_0/\eta\bar{u}$ across tube exit plane.

due to the surrounding medium were very low in comparison with viscous forces in both these sets of experiments, and the computational conditions, in which interfacial tension, inertia, and external drag are set equal to zero, are relevant.

The dominant feature in all these calculations is the remarkable stress singularity at the exit lip of the die; theoretically, an instantaneous switch takes place there from a very large shear stress to an even larger tensile stress at the outer edge of the jet. As one can see from figures 5(*d*)–(*f*), the stress field is remarkably complex, and is highly non-viscometric near the tube tip. In the present computation, one may cross-plot from figure 5(*e*), to find that the dimensionless shear stress along the tube wall changes from its Poiseuille-flow value of $-4{\cdot}0$ to larger magnitudes as the lip is approached close to the lip; the magnitude of the shear stress is given roughly by

$$t_{rz} = 1{\cdot}65\frac{\eta\bar{u}}{R_0 x^{\frac{1}{2}}}, \tag{5.1}$$

where x is the dimensionless distance from the tube lip inside the tube. Outside the tube, the shear stress at the surface is zero, but the tensile stress has the same form as (5.1), except that the numerical coefficient is about twice the value given there. In figure 7 we plot the dimensionless tensile stress $t_{zz}R_0/\eta\bar{u}$ at the tube exit. Since we have a tensile stress at the outer radius, and the total axial load is zero, it is inevitable that the axial stress near the axis of symmetry is compressive. It is also true that the pressure on the axis is positive at the exit plane (figure 5(*g*)), and extrapolation of the pressure at the wall does not yield a zero exit pressure. It seems likely that the compressive stresses on the axis are the most important factor directly affecting the swelling. There may be other factors; for example, the change of boundary conditions at the singularity might have required a change in stream direction to satisfy all conditions. However, following

Michael (1958), it is known that no change in direction is needed to satisfy all boundary conditions. By comparing the result of (4.2) for the pressure drop into (or out of) a tube from (or into) a large reservoir with the results of figure 5(*e*), we see that the rate of energy dissipation (above the Poiseuille losses) is only about 45 % of that given by (4.2).

6. Closure

The present work shows that the use of finite-element methods for free-surface viscous flow problems is elegant, and that results of acceptable accuracy can be produced with a reasonable expenditure of computing effort. The accuracy attained in a particular problem is clearly a function of the number of elements used and their distribution, which in turn governs the time for solution. In the stick–slip problem considered here, the primary variables u, w, and p are determined at a level better than 1% almost everywhere, but the stress components may be up to several per cent in error, especially near the singularity (see figure 4(*c*)). Overall quantities, such as pressure drop, are more accurate with only a fraction of a per cent error observed (compare (4.1) and (4.2)) for the inlet problem. For these problems one iteration with 135 elements (897 unknowns) consumed 5·16 minutes of central processing unit time on the IBM 360/67, but this time may be greatly reduced if lower accuracy is acceptable.

We have used the program to solve a difficult flow problem, which already gives us some insight into the type of problems that will be encountered in studying non-Newtonian die-swell. The presence of a stress singularity is inevitable in many of these problems, and the program must be able to handle it. The treatment of the convective acceleration terms is a subject of current research activity, and, with the addition of a time integration operator for transient problems (Taylor & Hood 1973), should create a powerful tool for analysis.

This work was partially supported by a National Science Foundation grant and by an Office of Naval Research grant at Brown University. Computing time was donated by the University Computing Centre.

REFERENCES

Atkinson, B., Brocklebank, M. P., Card, C. C. H. & Smith, J. M. 1969 Low Reynolds number developing flows. *A.I.Ch.E. J.* **15**, 548.

Atkinson, B., Card, C. C. & Irons, B. 1970 Application of the finite element method to creeping flow problems. *Trans. Inst. Chem. Eng.* **48**, T 276.

Batchelor, J. & Horsfall, F. 1971 Die swell in elastic and viscous fluids. *Rubber and Plastics Res. Assoc. of Great Britain, Res. Rep.* 189.

Chan, S. T. K. & Larock, B. E. 1973 Fluid flows from axisymmetric orifices and values. *Proc. A.S.C.E., J. Hydr. Div.* **99**, 81.

Cheng, R. T. 1972 Numerical solution of the Navier–Stokes equations by the finite element method. *Phys. Fluids*, **15**, 2098.

Felippa, C. A. 1966 Refined finite element analysis of linear and nonlinear two-dimensional structures. *University of California at Berkeley, Rep. SESM* 66–22.

Finlayson, B. A. 1972 Existence of variational principles for the Navier–Stokes equation. *Phys. Fluids*, **15**, 6.

FOX, D. G. & DEARDORFF, J. W. 1972 Computer methods for simulation of multidimensional nonlinear, subsonic, incompressible flow. *A.S.M.E. Paper*, 72-HT-61.

GAVIS, J. 1964 Contributions of surface tension of expansion and contraction of capillary jets. *Phys. Fluids*, **7**, 1097.

GOREN, S. L. & WRONSKI, S. 1966 The shape of low-speed capillary jets of Newtonian liquids. *J. Fluid Mech.* **25**, 185.

HERRMANN, L. R. 1965 Elasticity equations for incompressible and nearly incompressible materials by a variational theorem. *A.I.A.A. J.* **3**, 1896.

HORSFALL, F. 1971 A theoretical treatment of die swell in a Newtonian liquid. *Rubber and Plastics Res. Assoc. of Great Britain, Res. Rep.* no. 192.

HUH, C. & SCRIVEN, L. E. 1971 Hydrodynamic model of steady movement of a solid liquid fluid contact line. *J. Coll. Interface Sci.* **35**, 85.

KANTOROVICH, L. V. & KRYLOV, V. I. 1964 *Approximate Methods of Higher Analysis.* Wiley.

LODGE, A. S. 1964 *Elastic Liquids.* Academic.

MICHAEL, D. H. 1958 The separation of a viscous liquid at a straight edge. *Mathematika*, **5**, 82.

MIDDLEMAN, S. & GAVIS, J. 1961 Expansion and contraction of capillary jets of Newtonian liquids. *Phys. Fluids*, **4**, 355.

ODEN, J. T. 1970 Finite element analogue of Navier–Stokes equation *Proc. A.S.C.E., J. Engng Mech. Div.* **96**, 529.

ODEN, J. T. & WELLFORD, L. C. 1972 Analysis of flow of viscous fluids by the finite-element method. *A.I.A.A. J.* **10**, 1590.

OLSON, M. D. 1972 A variational finite element method for two-dimensional steady viscous flows. *Proc. Specialty Conf. on Finite Element Method in Civil Engineering, Engineering Institute of Canada, Montreal*, p. 585.

ORSZAG, S. A. 1971 Numerical simulation of incompressible flows within simple boundaries. I. Galerkin (spectral representation). *Studies in Appl. Math.* **50**, 293.

PRACHT, W. E. 1971 A numerical method for calculating transient creep flows. *J. Comp. Phys.* **7**, 46.

RICHARDSON, S. 1970*a* The die-swell phenomenon. *Rheol. Acta*, **9**, 193.

RICHARDSON, S. 1970*b* A 'stick–slip' problem related to the motion of a free jet of a low Reynolds numbers. *Proc. Camb. Phil. Soc.* **67**, 477.

SCHKADE, A. F. 1970 A refined axisymmetric finite element method for the analysis of nearly incompressible solids. Ph.D. dissertation, University of Texas at Austin.

SZABO, B. A. & LEE, G. C. 1969 Derivation of stiffness matrices for problems in plane elasticity by Galerkin's method. *Int. J. Num. Meth. Eng.* **1**, 301.

TANNER, R. I. 1963 End effects in falling-ball viscometry. *J. Fluid Mech.* **17**, 161.

TAYLOR, C. & HOOD, P. 1973 A numerical solution of the Navier–Stokes equations using the finite element technique. *Computers and Fluids*, **1**, 73.

THOMPSON, E. G., MACK, L. R. & LIN, F. S. 1969 Finite-element method for incompressible slow viscous flow with a free surface. *Developments in Mechanics*, **5**, 93.

WALDRON, K. J. 1966 M.S. thesis, University of Sydney.

WEISSBERG, H. L. 1962 End correction for slow viscous flow through long tubes. *Phys. Fluids*, **5**, 1033.

ZIDAN, M. 1969 Zur Rheologie des Spinnprozesses. *Rheol. Acta*, **8**, 89.

ZIENKIEWICZ, O. C. 1971 *The Finite Element Method in Engineering Science.* McGraw-Hill.

ZIENKIEWICZ, O. C. & TAYLOR, C. 1972 Weighted residual processes in F.E.M. with particular reference to some transient and coupled problems. *Lectures for NATO Advanced Study Institute.*